Investigation of Origin of Attached Cu-Ag Droplets to Solid Particles During High-Temperature Slag/Copper/Spinel Interactions

INGE BELLEMANS, EVELIEN DEWILDE, BART BLANPAIN, NELE MOELANS, and KIM VERBEKEN

This study investigates the origin of mechanically entrained metal droplets in liquid slag due to their interaction with solid spinel particles. Two possible mechanisms were proposed previously: separately formed droplets and spinel particles get attached to each other due to agitation of the slag and metal phases; or the spinel particles form by a chemical reaction together with a new droplet or alongside a droplet that was already present in the system. In this study, an inert tracer element was added to the metallic phase in adapted sessile drop experiments. For this purpose, Cu-Ag alloys, with various Ag-contents, were produced. The results showed that the small entrained metal droplets within the slag droplet contained Ag, but in very low amounts with respect to the amount of Ag in the Cu-Ag alloy. This indicates that the entrained metal droplets are formed due to a sequential combination of the two origins: first, very small metal droplets are dispersed in the slag drop, due to the emulsification process. Then, these metal droplets are nucleation sites for the Cu-spinel reactive formation.

DOI: 10.1007/s11663-017-1088-4

I. INTRODUCTION

THE overall metal recovery in primary and secondary copper production is limited by copper droplet losses.[1] Limiting these metal losses requires a fundamental understanding of their characteristics and origin. Copper losses in slags are in literature generally subdivided into chemical and mechanical losses.[2–4] Chemical copper losses represent the formation and dissolution of copper sulfide and/or copper oxide and are inherent to pyrometallurgical processes. The chemical losses are linked to the system's thermodynamics, *i.e.*, the oxygen partial pressure,[2,4–6] the temperature, and the composition of the slag and matte.[2,4–6]

Mechanically entrained copper refers to entrapped or floating unsettled droplets. In primary copper production, these include both matte and metal droplets, whereas mainly metallic droplets are entrapped in secondary copper production. For secondary production, which is based on for example e-scrap, some noble metals are also collected in the metallic phase and even though these noble metals have limited solubility, their loss has a potentially significant economic impact. One of the causes of the mechanical entrainment of the droplets is the precipitation of copper or matte droplets within the slag due to a decrease in the solubility of copper in the slag. This decrease finds its origin in the inhomogeneity of the process, *e.g.*, there are zones with a different local oxygen potential or a lower temperature.[7] A second cause of the mechanical entrainment is the dispersion of metal into the slag by gas-producing reactions. Minto and Davenport[8] suggested that SO_2 bubbles nucleated at the bottom of the furnace rise to the matte/slag interface and elevate a surface film of matte into the slag.[7,8] This surface film can break down because of capillary instability, dispersing fine droplets into the slag. Operational actions performed in pyrometallurgical processes, such as tapping or charging, are another possible cause for mechanically entrained droplets. During tapping, the denser liquid can rise when flowing around obstacles in the vessel and hence mechanical entrainment can take place.[3] Moreover, gas injections, turbulence, or pouring of one phase into the other can cause the physical dispersion of the denser layer into the slag.[3,9]

These causes were already examined and discussed extensively in literature, but another possible source for

INGE BELLEMANS and KIM VERBEKEN are with the Department of Materials, Textiles and Chemical Engineering, Ghent University, Technologiepark 903, Zwijnaarde, 9052 Ghent, Belgium. Contact e-mail: Kim.Verbeken@UGent.be EVELIEN DE WILDE is with Umicore R&D, Kasteelstraat 7, 2250 Olen, Belgium. BART BLANPAIN and NELE MOELANS are with the Department of Materials Engineering, KU Leuven, Kasteelpark Arenberg 44, Bus 2450, Heverlee, 3001 Leuven, Belgium.

Manuscript submitted December 28, 2016.

Published online: 02 October 2017

the mechanical entrainment of copper droplets is often not taken into account: the attachment of droplets to solids in slags, hampering their sedimentation. These solids have often been found to have a spinel structure and their attachment to metal droplets was reported by Ip and Toguri[7] and Andrews.[9] This attachment was investigated in a synthetic slag system in our previous work.[10] Although the phenomenon was clearly observed, limited experimental or industrial data are available and more fundamental insight is an absolute prerequisite to be able to avoid this type of metal loss.[5] Apart from experimental efforts, the phase field modeling approach has been used as well to gain insights into the responsible mechanisms.[11–13]

As suggested in previous work by De Wilde *et al.*,[14,15] sticking droplets can originate from a chemical reaction. Possible reaction schemes were proposed: a first in which the spinel solids and copper droplets form together due to a simultaneous reduction of copper oxides into metallic copper and oxidation of slag oxides into more stable spinel structures; and a second, in which the spinel solids form by heterogeneous nucleation on an already present Cu droplet in an analogous way.

In De Wilde *et al.*'s previous work,[15] the interaction between $MgAl_2O_4$, a copper droplet and a synthetic PbO-based slag were studied using an adapted sessile drop experiment to focus on the simultaneous copper-spinel-slag interaction. During the experiment, the copper droplet moved towards the slag droplet and a certain emulsification took place between the slag and copper droplet, after which the copper droplet positioned itself on top of the slag droplet. An extensive microstructural study was performed afterwards to study the spinel-copper-slag interactions. Within the slag droplet, small entrained copper droplets were observed to be attached to spinel particles. A reactive origin was proposed: the spinel solids and copper droplets form together due to a simultaneous reduction of copper oxides into metallic copper and the oxidation of slag oxides into more stable spinel structures. As spinel solids are characterized by very fast formation rates, new spinel solids can form directly next to the metallic copper droplets, leading to copper droplets, which are attached to spinel solids. However, the presence of the small metal droplets within the large slag droplet could also find its origin in the emulsification step.

The aim of this work was to investigate this hypothesis. Therefore, additional experiments with the adapted sessile drop set-up were performed. Moreover, several Cu-Ag alloys were used as Ag fulfilled the role of a tracer element. Ag is very noble and very unlikely to undergo oxidation, and thus it will remain in the metallic phase. If the small metal droplets within the large slag droplet do not contain the tracer element, this confirms the fully reactive origin hypothesis. However, if the tracer element is observed within the small metal droplets in the large slag droplet, these small metal droplets originated fully or partially from the emulsification step. Moreover, as a combined dispersive-reactive origin would result in lower Ag-contents in the smaller droplets than in the large metal droplet, several Ag-contents in the alloys were used to investigate this possibility.

II. EXPERIMENTAL PROCEDURE

A. *Production of the Slag System*

The same industrially relevant synthetic slag system (PbO-CaO-SiO_2-Cu_2O-Al_2O_3-FeO-ZnO) as previously used[15] was employed. It was produced by melting oxides of appropriate quantities, corresponding to a slag composition in the spinel primary phase field. The targeted slag composition is shown in Table I. FeO was added as a combination of metallic iron and hematite and CaO was added as limestone. 400 g of the targeted composition was weighed, mixed, and transferred in an Al_2O_3 crucible (270 mL). The Al_2O_3 crucible, surrounded by a protective SiC crucible, was heated in an inductive furnace (Indutherm, MU3000) up to a temperature of 1073 K (800 °C), under a protective N_2 atmosphere above the bath. At 1073 K (800 °C), the N_2 atmosphere was replaced by a CO/air mixture with volume ratio of 1 to 2.36, corresponding to an oxygen partial pressure (p_{O_2}) of 10^{-7} atm, with a total flow rate of 60 l/h. This atmosphere was kept constant during the remainder of the experiment. The slag was heated to 1473 K (1200 °C) and this temperature was kept for 30 minutes to melt all components. Subsequently, N_2 (60 l/h) was bubbled through the slag for homogenization purposes. Afterwards, the induction furnace was kept at 1473 K (1200 °C) for 150 minutes. The high-temperature state of the system (*i.e.*, a mixture of slag/spinel/droplets) was obtained using a cold sampling bar, which was directly quenched in water and subsequently dried in a dry chamber at 423 K (150 °C).

A representative sample of the quenched slag obtained after 150-minute equilibration at 1473 K (1200 °C) was investigated microscopically previously.[15] Three phases were observed: slag (SL), spinel (SP), and copper droplets (Cu-dr). Some of the present copper droplets display a sticking behavior to spinel particles. The spinel often had a border richer in Fe with respect to the core, which was generally richer in Al. Similarly, the Cu-droplets often had a Pb-rich border. The various phases present in the system are illustrated in Figure 1. WDS analysis was also performed on the various phases. The resulting compositions are summarized in Table II.

The composition of the slag itself was different compared to the targeted composition in Table I. For Cu, this difference can be explained by the formation of alloy droplets within the slag phase. Moreover, Pb will dissolve mostly in the alloy phase rather than in the slag phase, in accordance with the findings of Takeda *et al.*,[16] resulting in a lower PbO content of the slag (see Table II). Takeda *et al.*[16] also showed that Zn dissolves more in the slag phase, but the amount of ZnO in Table II is lower than the start composition given in Table I, as it is one of the major spinel-forming components. The spinel solids consist of the three spinel

Table I. Selected Targeted Synthetic Slag Composition Based on Thermodynamic Calculations with FactSage (FactPS and FTOxid Database; Input: 100 g of the Composition in Table I; Selection of All Possible Pure Compound Species and All Solution Species; Conditions: 1473 K (1200 °C), 1 atm Total Pressure and Fixed Partial Pressure of O_2 of 10^{-7}; Resulting in Three Phases at Equilibrium: Liquid Metallic Copper Phase, Liquid Slag Phase, and Solid Spinel Phase)

	ZnO	PbO	SiO_2	Al_2O_3	Cu	CaO	FeO
Wt Pct	6.5	39.3	13.8	7.3	3.9	9.8	19.4

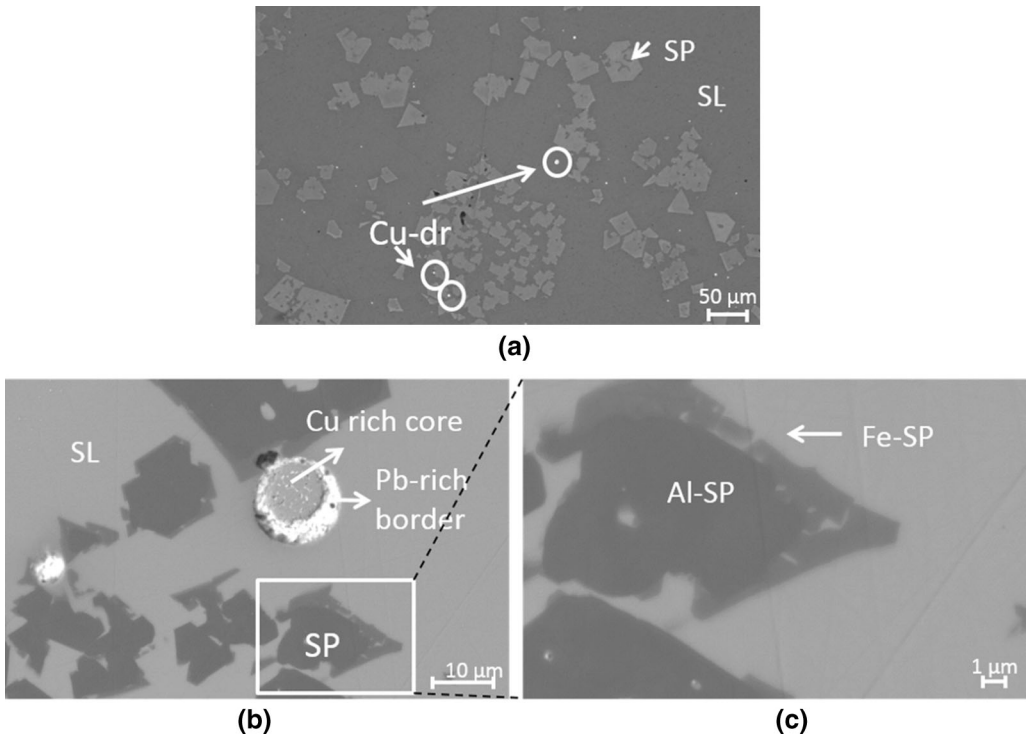

Fig. 1—Representative LOM (*a*) and BSE (*b*, *c*) images of quenched slag system obtained after 150-minute equilibration at 1473 K (1200 °C). (SP = spinel, SL = slag, Cu-dr = Cu-alloy droplets, Al-SP = Al-rich spinel phase, Fe-SP = Fe-rich spinel phase).[15]

Table II. Overview WDS Analysis of the Slag, Fe-Rich Spinel Phase, Al-Rich Spinel Phase, and Cu-Rich Core and the Pb-Rich Border of the Present Cu-Pb Alloy Droplets[15]

Wt Pct	Al_2O_3	'FeO'	'Cu_2O'	CaO	ZnO	PbO	SiO_2
Slag	7.1	16.1	1.3	8.7	5.5	36.4	25.7
Al-rich spinel	36.9	39.7	0	0	22.5	0.1	0.2
Fe-rich spinel	17.7	63.6	0.1	0	14.3	0.3	0.4

Wt Pct	O	Al	Fe	Cu	Ca	Zn	Pb
Cu core	0.7	0	1.5	95.1	0	0.5	1.2
Pb-rich border	3.4	0	1.4	1.9	0.1	0.9	92.3

forming components in the slag (*i.e.*, 'FeO', ZnO, and Al_2O_3). Some of the spinel particles consist of two phases, namely an Fe-rich spinel phase at the border (Fe-SP) and an Al-rich spinel phase in the core (Al-SP) of the particle. Other spinel particles consist completely of the Fe-rich spinel phase. Under the present experimental conditions, Cu-Pb droplets with a phase separation between a Cu-rich core and a Pb-rich border are formed. The phase separation is a direct consequence of the low Pb solubility in Cu at lower temperatures, and therefore, this phase separation is expected not to be present at the high temperature during the experiment.

B. *Spinel Preparation*

Spinel ($MgAl_2O_4$) substrates were produced in a similar way as in the previous work,[15] using a spark plasma sintering equipment (type HP D25/1, FCT

system Rauenstein, Germany, equipped with a 250 kN uniaxial press)). The $MgAl_2O_4$ powder (Sigma Aldrich, spinel nano powder, <50 nm particle size) was sintered at a temperature of 1573 K (1300 °C) under a load of 60 MPa. Subsequently, the sintered spinel plates were annealed at 1273 K (1000 °C) for 3 hours and were in a final step polished to a mirror finish using 9, 3, and 1 μm diamond pastes. The spinel phase was confirmed by XRD analysis, while some additional small corundum peaks were present in the XRD spectrum as well (Siemens diffractometer D5000). The roughness parameter R_A of the $MgAl_2O_4$ substrates has an average value of 0.19 ± 0.08 μm (Talysurf profilometer).

C. *Alloy Production*

The Cu-Ag-alloys were produced using an inductive microgranulation furnace (Indutherm, GU500), allowing the production of granules with proper dimensions for the contact angle measurements. Four different Cu-Ag alloys were produced, containing, respectively, 5 wt pct Ag, 12.5 wt pct Ag, 20 wt pct Ag, and 30 wt pct Ag. Appropriate amounts of the metals were weighed and melted under a protective Ar-atmosphere in graphite crucibles. Once molten, the high-frequency magnetic field ensured mixing of the alloying elements during 15 minutes. Subsequently, the alloy was granulated into small granules.

D. *Sessile Drop Experiments*

1. *Set-up*

The interaction between $MgAl_2O_4$ and copper or slag was studied using an infrared heating furnace, included in the confocal scanning laser microscopy set-up (Lasertec 1LM21-SVF17SP, CSLM). The infrared heating furnace allows fast heating and cooling with a 1.5 kW halogen lamp placed in the lower focal point of a small Au-coated gastight ellipsoidal chamber that reflects the light to the other focal point where the observed sample is positioned. A programmable PID controls the temperature, read from a type B (Pt-6 pct Rh/Pt-30 pct Rh) thermocouple, which is part of the sample holder. It should be noted that the correct temperature can only be measured at temperatures above 673 K (400 °C). As the sample holder is made of Pt-Rh which is part of the thermocouple, the measured temperature is very representative for the actual temperature of the sample. Nonetheless, a small difference is present due to the fact that the spinel substrate has a certain thickness. The Cu-Ag and slag particle on top of the substrate consequently have a slightly lower temperature than the one measured. To quantify the difference between the actual temperature in the Cu-alloy droplet and temperature measured by the thermocouple, an initial test was performed with pure Cu on a $MgAl_2O_4$ substrate under a purified Ar flow, for which following temperature profile was used: heating to 573 K (50 K/min), maintaining the temperature for 1 minute, heating to 1343 K (200 K/min) and maintaining the temperature for 1 minute, heating to 1523 K (10 K/min) and maintaining the temperature for 15 minutes, cooling down to room temperature (500 K/min). Pure Cu was observed to melt at approximately 1409 K, indicating that there is a temperature difference of approximately 53 K between the actual temperature and the displayed temperature. This temperature difference was taken into account for all the sessile drop experiments using this set-up. It should, however, be noted that small differences, attributed to the age of the halogen lamp, may also arise between the actual temperature and the displayed temperature.

An extra window is placed on the side of the heating chamber, allowing to monitor the wetting of the droplet on the substrate, which is recorded with a camera (Ganz ZC-F10C3), placed on the same height. An oxygen gas analyser in the gas outlet monitors p_{O_2} variations in the heating chamber (Cambridge Sensotec LTD, Rapidox 2100).

2. *Performed experiment*

The simultaneous interaction of copper and slag with a $MgAl_2O_4$ substrate was evaluated under a protective Ar atmosphere. Before the start of the experiment, the $MgAl_2O_4$ substrate was cleaned ultrasonically in acetone, and the copper was etched using a $1H_2O$:1HCl solution, to remove the outer copper oxide layer. The $MgAl_2O_4$ substrate was placed on the sample holder and leveled carefully. Subsequently, both copper and slag were placed on the substrate. The heating chamber was closed and flushed three times with Ar. First, the temperature was raised to 573 K (300 °C), with a heating rate of 50 K/min. After 1 minute at 573 K (300 °C), the temperature was increased further to 1173 K (900 °C), with a heating rate of 200 K/min. After 1 minute at 1173 K (900 °C), the chamber was further heated to 1523 K (1250 °C), which was maintained for 8 minutes. Finally, the sample was cooled down with a cooling rate of 500 K/min. The complete process, starting from the melting of the droplet until the final cooling, was monitored.

Special care was taken to assure that the masses of the slag and copper alloy were very similar. The average weights of slag and copper alloys during the experiments were 0.0269 ± 0.0041 and 0.0265 ± 0.0048 g, respectively. The experiment was repeated multiple times to ensure the reproducibility of the observations and to investigate whether the wt pct Ag in the Cu-Ag alloys has a certain influence. The monitored p_{O_2} value during the experiments was of the order of $1.5 \times 10^{-5} \pm 1$ at. pct.

The obtained sessile drop samples were analyzed using light optical microscopy (LOM, Keyence VHX-S90BE) and electron probe microanalysis, using the secondary electron (SE) microscopy mode (SEM-SE, FEI Quanta 450 with field emission gun). For the latter, the sample was coated with a conductive carbon layer. The composition of the different phases is analyzed using energy dispersive spectroscopy (SEM-EDX, FEI Quanta 450 with field emission gun, 20 kV).

III. RESULTS AND DISCUSSION

A. *Melting, Wetting, and Interaction Behavior of Copper Alloy and Slag on $MgAl_2O_4$*

A typical example of the melting and wetting behavior of slag and copper on a spinel substrate is presented in Figure 2 using the captured video images obtained during the experiment. The moment at which the slag starts to melt is considered as the start of the experiment and is chosen as zero-point for the timescale of the experiment ($t_{melt\ slag} = t_{start} = 0$ second). It should be noted that the images of Figure 2 were slightly adapted in contrast and brightness to make the slag and copper droplet more visible. These phases were not clearly visible, because the extra side-window of the heating chamber used for the sideways observation was obscured. This was done because the sample emits too much light at the higher temperatures [1523 K (1250 °C)], which would make the interaction at higher temperatures not visible.

Different stages during the experiment can be distinguished, as indicated on Figure 2. First, the slag droplet melts, followed by the melting of the copper alloy. Usually, as the viscosity of molten metals is very low, the time needed for millimetric size droplets to reach capillary equilibrium in non-reactive systems is less than 10^{-1} seconds, whereas the spreading times in reactive metal/ceramic systems, usually lay in the range of 10^{1}-10 seconds and these systems are typically controlled by the interfacial reaction itself.[17] Once the slag is completely molten, a good wetting with the spinel substrate is observed. The apparent contact angle is 25.9 ± 1.7 deg. The copper alloy, on the other hand, is almost spherical with an apparent contact angle of 118.5 ± 1.4 deg, indicating a very low wettability of the alloy on the spinel. This wetting behavior is in good correspondence with previous observations by De Wilde *et al.*[18] The wetting behavior of the slag with respect to the spinel appears to be much higher than that of the alloy. The slag gradually spreads on the spinel substrate and eventually reaches the copper droplet, which continuously keeps it spherical shape.

After 85 seconds, the slag touches the copper droplet. Once this takes place, the copper moves on top of the

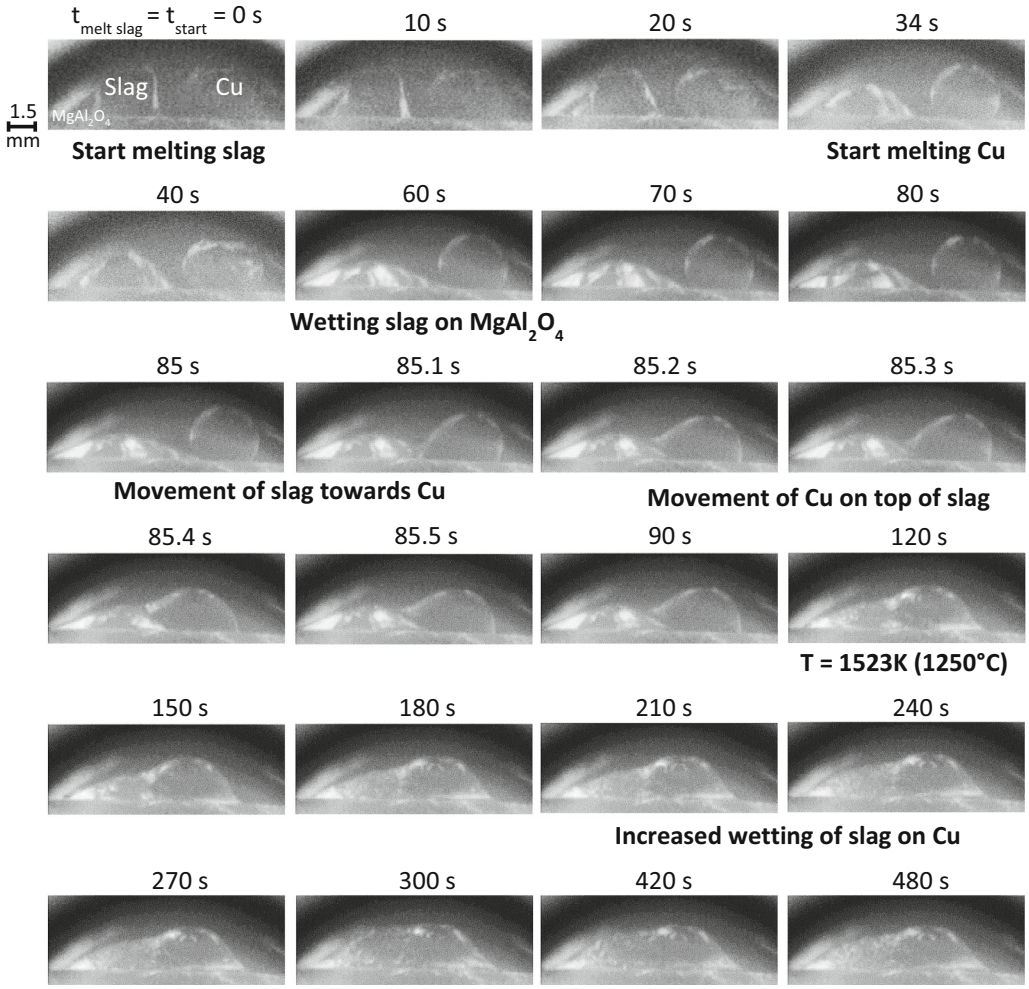

Fig. 2—Captured images during the high-temperature CSLM experiment with Cu-20 wt pct Ag. Above each image, the time in seconds is shown, where the melting point of the slag is taken as the zero-point for the timescale ($t_{melt\ slag} = t_{start} = t_0$). Different stages were defined within the melting and heating process: melting of the slag; melting of the copper; wetting of slag on the substrate; movement of the slag towards the Cu; movement of the Cu on top of the slag and increased wetting of slag on top of the Cu.

slag very rapidly, *i.e.*, in about half a second. After this stage, the liquid copper stays on top of the slag and this image gives the impression that the copper droplet is not in contact with the $MgAl_2O_4$ substrate. Based on the densities of copper and slag, the opposite behavior would be expected. It should be noted that due to the very low masses of slag and copper used in the sessile drop experiment, the gravity effect on the droplets is limited and it can be assumed that the interfacial energies between the spinel substrate and both liquids will be the dominant factor in our experiment.[19]

After the movement of the copper on top of the slag, during the interaction time of 8 minutes at 1523 K (1250 °C), the slag starts to wet the copper droplet, which lies on top of the slag. This is particularly visible when considering the height of the left side of the slag with respect to the height of the copper droplet on top of the slag. First, the copper droplet is clearly situated in a higher position, but in the end of the experiment, the slag on the left side reached the same height.

Because the movement of the copper on top of the slag happens so fast, the small metal droplets attached to spinel particles that were observed in the slag phase in similar experiments previously[15] might result from this fast 'sweeping' of the slag in between the copper alloy droplet and the spinel substrate. This is why, in this study, copper-silver alloy droplets were used. If the mechanically entrained copper alloy droplets have the same composition as the large alloy droplet, the origin of the attachment of the small copper droplets to the solid spinel particles lies in the fast mixing of the two phases during the movement of the copper on top of the slag. However, when the attached copper alloy droplets have a different composition than the large alloy droplet, this would be a strong indication that the entrainment of the copper droplets has a reactive origin, as was proposed in previous work.[14,15] If the small metal droplets within the large slag droplet do not contain the tracer element Ag at all, the origin can be stated as fully reactive. If the concentration of the tracer element is less than the large alloy droplet, a combined origin would be responsible for the mechanically entrained small droplets.

The adapted sessile drop experiment allowed the simultaneous study of the interactions between both liquid slag and liquid copper with a solid spinel $MgAl_2O_4$ substrate. Consequently, the relevant interactions that determine the phenomenon of sticking copper droplets in slags will be examined in the next section. The microstructures and compositions of different regions within the high-temperature CSLM samples are examined for the different Ag alloys.

B. *Microstructural Analysis*

1. *General overview*

The LOM images of the cross section of the $MgAl_2O_4$-slag-Cu (30 wt pct) Ag sample are shown in Figure 3. Central in this figure, a global overview is shown, surrounded by more detailed micrographs of several regions in the cross section. Similar results were obtained for the other Cu-Ag alloys.

The general overview image (central in Figure 3) confirms that there is no direct contact between the $MgAl_2O_4$ substrate and the large copper droplet. The large Cu-Ag droplet has undergone a certain phase separation during the cooling down, as the Cu-Ag phase diagram predicts one completely liquid Cu-Ag phase at high temperatures, but a phase separation between a Cu-rich and a Ag-rich phase at temperatures below the eutectic temperature of 1052 K (779 °C).

The slag situated close to the large copper alloy droplet contains several small metal droplets attached to spinel particles within the slag. Further away from the large copper alloy droplet, smaller non-attached metal droplets are also present alongside finely dispersed spinel solids. In the outer regions of the slag phase, less or almost no metallic droplets are observed. Underneath the large copper alloy droplet, a very thin interaction layer can be observed. However, it is immediately clear that this slag layer is much thinner (on the order of 10 μm) than in the previous work[15] (on the order of 100 μm). The different zones were also investigated with SEM-EDX and are discussed into more detail in the following sections.

2. *Large alloy drop*

The phase separation within the large droplet can be observed by both the SE images and the elemental maps in Figure 4. The Cu-Ag alloy clearly separates into a copper-rich and a silver-rich phase. The average measured composition of the complete droplets and the compositions of the separate phases for the 20 and 30 wt pct Ag alloys are shown in Table III. Only the amounts of Cu and Ag are presented here, because the other elements were detected in amounts lower than the error of the measurement.

The Ag-rich phase in the 20 wt pct Ag alloy could not be measured accurately due to the limits of spatial resolution of the EDX. However, it is clear that such an Ag-rich phase is present, as the SE images clearly indicate this and the average composition has more Ag than the Cu-rich phase.

The Cu-Ag phase diagram, calculated with the Factsage thermodynamic software,[20] predicts a homogeneous liquid Cu-Ag phase at 1523 K (1250 °C). Upon cooling, a phase separation occurs which shows characteristics of spinodal decomposition instead of a nucleation and growth mechanism.[21] Therefore, the temperature at which the alloy droplet solidified and simultaneously decomposed spinodally can be approximated by a Factsage calculation which fits the observed phase compositions to the theoretical ones. The compositions of the two measured phases correspond to the equilibrium situation at a temperature of 1003 K (730 °C) and 1051 K (778 °C), respectively, where the latter temperature is the eutectic temperature (the temperature at which the last liquid phase disappears under equilibrium cooling).

3. *Slag at the side of large alloy drop*

An overview of the microstructures at the side of the large metal droplet for the different Cu-Ag alloys is given in Figure 5. For the 5, 12.5, and 30 wt pct Ag alloys, the microstructures are similar and contain metal

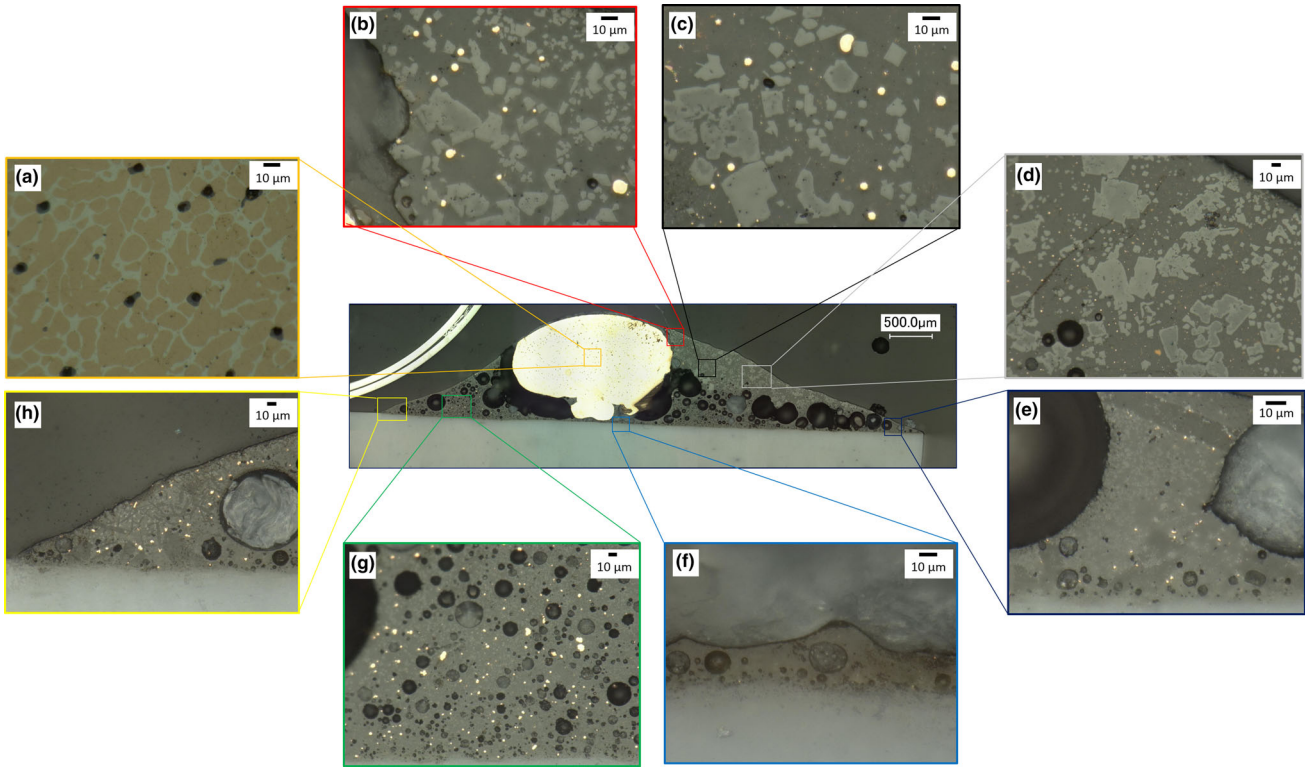

Fig. 3—LOM of the cross section of the $MgAl_2O_4$-slag-Cu (30 wt pct) Ag sessile drop sample. (central) General overview of slag droplet and copper droplet on the substrate. (surrounding) Detailed overview of the microstructure within the copper or slag droplet: (*a*) large alloy drop; (*b*) slag at the side of the large alloy drop; (*c*) slag further away from the large alloy drop; (*d*, *e*) slag far away from the large allay drop; (*f*) slag-spinel substrate interface; (*g*) slag further away from the large alloy drop; (*h*) slag far away from the large allay drop.

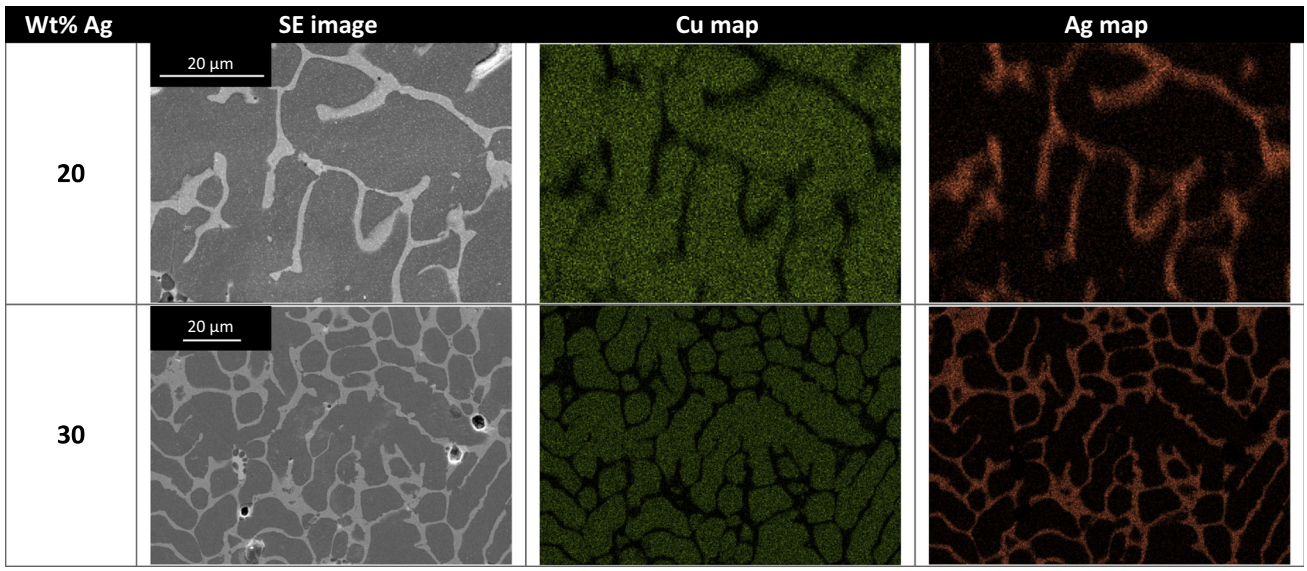

Fig. 4—SE images and Cu and Ag EDX-maps illustrating the phase separation within the large Cu-Ag droplet.

Table III. Average Measured Composition of the Complete Droplets and the Compositions of the Separate Phases for the 20 and 30 Wt Pct Ag Alloys

Proposed Wt Pct Ag	Measured Average Composition	Composition of Ag-Rich Phase	Composition of Cu-Rich Phase
20	17.2 wt pct Ag	—	94.7 wt pct Cu and 5.3 wt pct Ag
30	22.2 wt pct Ag	18.4 wt pct Cu and 81.6 wt pct Ag	94.4 wt pct Cu and 5.6 wt pct Ag

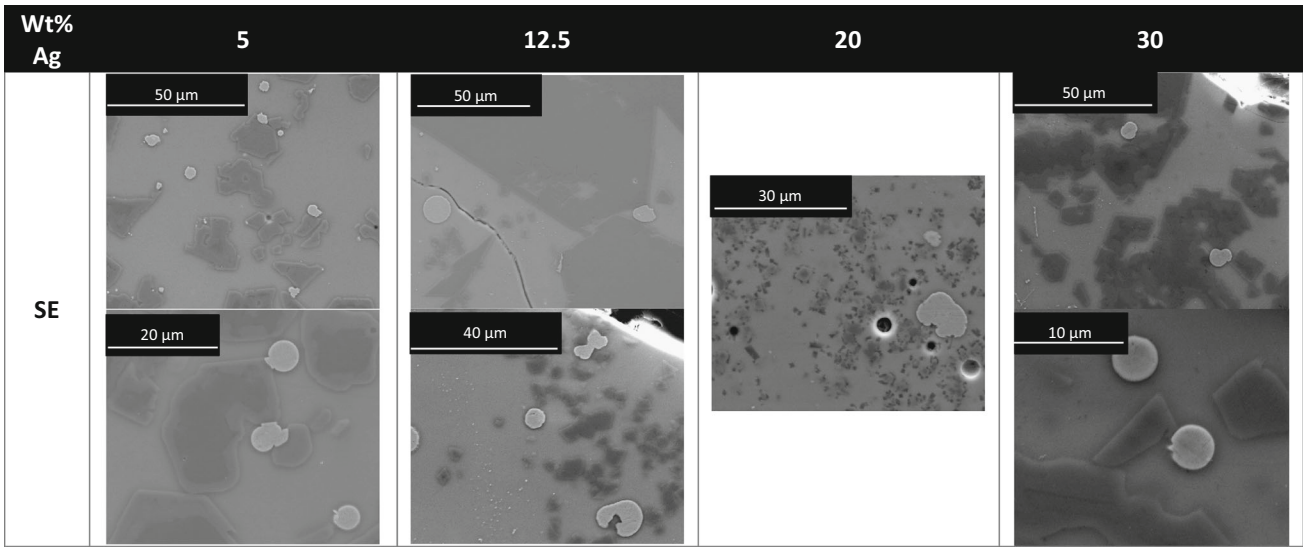

Fig. 5—SE images of the microstructures at the side of the large copper alloy droplet for the different Cu-Ag alloys.

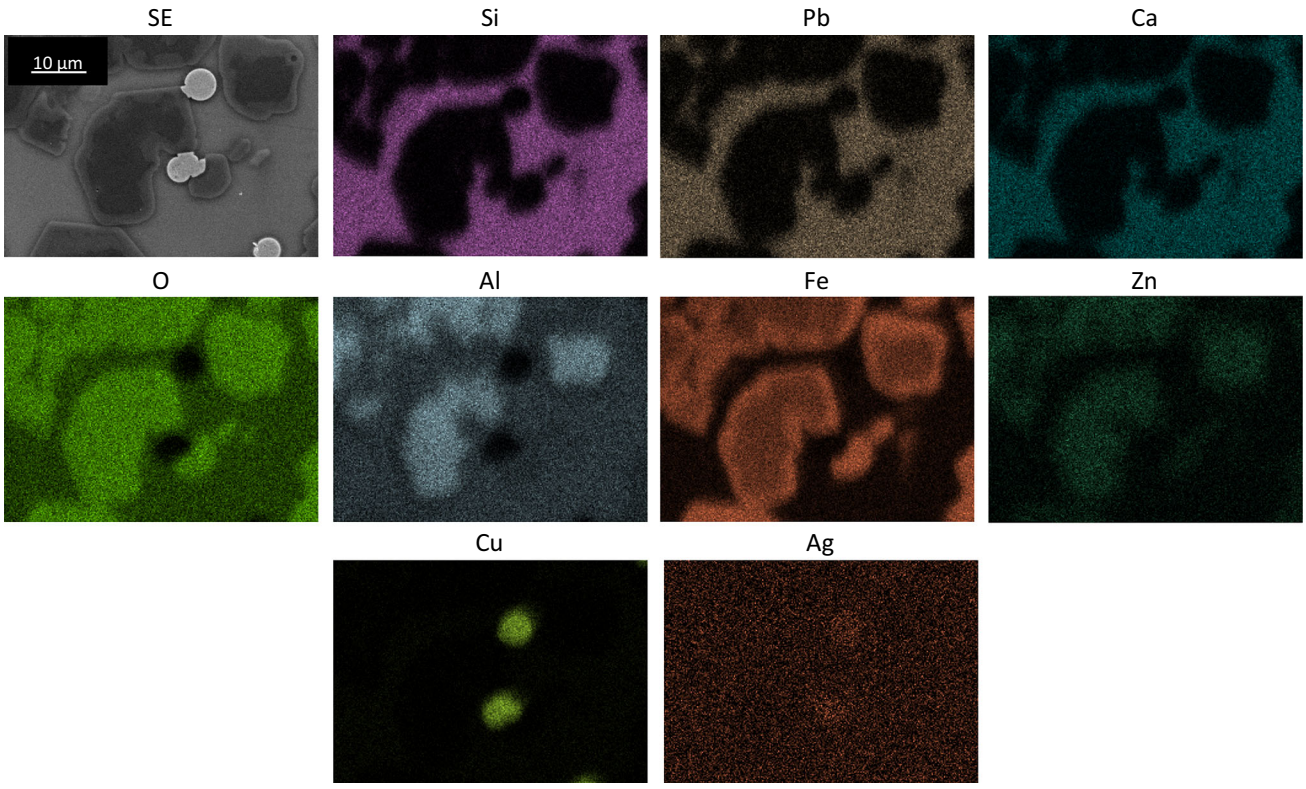

Fig. 6—Elemental map of the microstructure next to the large Cu-5 wt pct Ag droplet.

droplets attached to solid spinel particles in the slag phase. This is not the case for the 20 wt pct Ag alloy, where small darker solids are also present. An elemental map of an attached droplet for the 5 wt pct Ag sample is shown in Figure 6.

It is clear from this map that the spinel forming elements are O, Al, Fe, and Zn. Si, Pb, and Ca only appear inside the slag phase while the metal droplets consist of Cu and Ag. The latter is more clear for the 30 wt pct Ag alloy, as shown in Figure 7. In Figure 6, it is also shown that the spinel particle has a core which contains Fe, Al, and Zn, but the border of the particle clearly contains a higher concentration of Fe. Quantitatively, this is also reflected in the compositions obtained by EDX measurements, as summarized in Table IV.

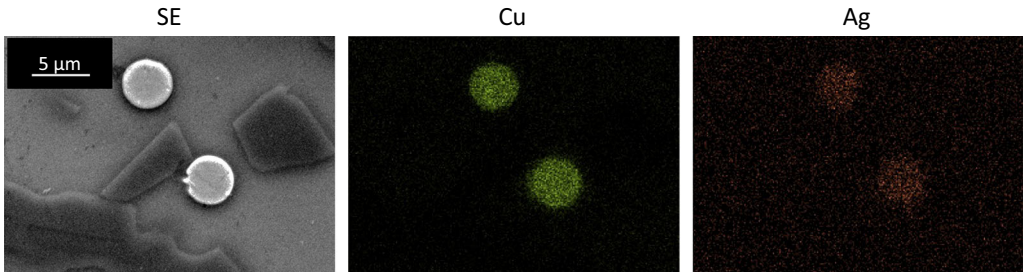

Fig. 7—Elemental map of the attached metal droplets next to the large Cu-30 wt pct Ag droplet.

Table IV. Average Measured Compositions for the Various Phases in the Microstructure at the Side of the Large Alloy for the Different Cu-Ag Alloys

Sample	Phase	Wt Pct Si	Wt Pct Pb	Wt Pct Ca	Wt Pct Mg	Wt Pct O	Wt Pct Al	Wt Pct Fe	Wt Pct Zn	Wt Pct Cu	Wt Pct Ag
5	slag	17.0	14.6	7.2	—	31.7	6.5	19.4	4.4	2.5	—
	inner spinel	—	—	—	—	30.9	12.8	42.0	12.7	—	—
	outer spinel	9.7	10.6	5.6	—	26.5	5.6	18.2	3.8	19.2	—
	attached Cu	—	—	—	—	5.3	1.9	4.1	1.1	79.3	—
	non-attached Cu	—	—	—	—	—	—	2.0	—	94.2	1.0
12.5	slag	14.9	23.4	8.5	—	30.2	6.3	7.1	1.9	6.9	—
	inner spinel	—	—	—	—	28.2	5.2	50.2	14.7	—	—
	outer spinel	1.1	1.4	—	1.1	30.4	7.7	46.2	10.0	1.5	—
	attached Cu	—	—	—	—	—	—	2.6	—	90.6	3.0
	non-attached Cu	—	—	—	—	—	—	—	—	94.5	2.6
	other solids	2.6	3.3	1.4	—	11.2	2.6	11.2	2.8	61.3	2.8
20	slag	15.9	23.6	9.0	—	29.9	6.8	5.0	1.4	7.3	—
	outer spinel	1.4	1.6	1.0	2.8	31.6	15.1	32.8	12.2	1.4	—
	attached Cu	2.1	3.5	1.5	—	1.5	1.1	1.5	—	84.3	3.2
	other solids	16.0	13.1	12.5	1.7	34.9	7.2	11.1	1.1	2.3	—
30	slag	15.8	24.7	8.7	—	30.3	6.0	6.5	2.4	5.0	—
	inner spinel	—	—	—	—	30.7	10.8	44.1	11.8	—	—
	outer spinel	2.1	2.3	—	—	30.6	11.3	39.4	11.5	1.2	—
	attached Cu	—	—	—	—	—	—	2.8	—	88.6	6.0

Compositions below 1 wt pct were assigned with '—'.

These measurements show that Pb, Si, and Ca are mainly present in the slag. Mg, which could only come from diffusion from the substrate, is nearly always measured in concentrations below the detection limit. The spinel particles mainly consist of O, Al, Fe, and Zn while the outer rim of the spinel clearly contains less Al and Zn. However, the amount of Fe also seems lower, as opposed to what is expected from the elemental map in Figure 6. Moreover, the amounts of the slag forming elements are also higher. This is probably due to the interaction volume (a depth of 1.93 μm and width of 1.49 μm can be estimated from Reference 22 with an accelerating voltage of 20 kV and a density estimated with an additive method to be 4.624 g/cm^3) inherent to SEM-EDX measurements and the fact that the spinel border is very thin and thus has slag underneath it, which will be measured by the EDX as well.

The metal droplets within the slag phase, either attached or non-attached, clearly contain Ag. They contain, however, less Ag than the proposed and actually measured (cfr. Table III) Ag content. The Ag content in the slag or the spinel phases is mostly below the detection limit as Ag mainly resides in the metal phase. The amount of Ag in the attached Cu droplets increases with the increasing Ag content in the Cu-Ag alloy. The attached metal droplets have a higher fraction of other elements (mainly Fe) than the non-attached metal droplets which could be related to secondary X-ray fluorescence: After a characteristic X-ray is emitted, it can be absorbed again by an atom in the sample and then, the absorbing atom is excited and subsequently relaxes, emitting its own characteristic X-rays. This is called secondary fluorescence. Because X-rays (primary or secondary) can travel relatively large distances through the sample, it is possible that the secondary emission process may occur at a location remote from that of primary emission, further degrading the spatial resolution of the X-ray signal. This secondary fluorescence of X-ray spectra of small Cu-particles in Fe-containing slags was already investigated and modeled with Monte Carlo simulations.[23]

The behavior of the slag and the copper alloy droplet on the $MgAl_2O_4$ substrate during the high-temperature CSLM experiment (Figure 2) indicates that the

copper-$MgAl_2O_4$ interaction is not stable in the presence of a slag phase. This seems to be in contradiction with the presence of the small entrained sticking copper droplets in the slag droplet, and with the observations of the attached droplets in slags in the previous work of De Wilde *et al.*[14] In Reference 15, it was already demonstrated that an attached copper droplet is more stable than a non-attached droplet from a thermodynamic point of view, assuming that the surface of the droplet does not change after the attachment, when the following condition is valid[14]: $\gamma_{SL\text{-}Cu} + \gamma_{SP\text{-}SL} \geq \gamma_{SP\text{-}Cu}$, with $\gamma_{SL\text{-}Cu}$ the slag-copper interfacial energy, $\gamma_{SP\text{-}SL}$ the spinel-slag interfacial energy, and $\gamma_{SP\text{-}Cu}$ the spinel-copper interfacial energy.

Unfortunately, at present, only limited data are available on $\gamma_{SL\text{-}Cu}$ for calcium ferrite slags,[24] and, to our knowledge, no data are available for $\gamma_{SP\text{-}Cu}$ or $\gamma_{SP\text{-}SL}$. However, it was already shown that the spinel composition influences the wetting behavior of copper alloys[25]: the contact angle of copper on $ZnFe_2O_4$ substrates (88 deg) was lower than on $MgAl_2O_4$ substrates (123 deg). The composition of the small spinel particles within the slag in our experiment is more related to the $ZnFe_2O_4$ substrate, and thus the attachment of small alloy droplets within the slag is thermodynamically feasible and not in contradiction with the non-wetting behavior of the large copper-alloy droplet on the $MgAl_2O_4$ substrate.

On the other hand, the origin of sticking droplets was proposed to be found in a chemical reaction, as elaborated in References 14 and 15. It is suggested that dissolved Cu can precipitate by reduction of the copper oxide, while the iron oxides in the slag next to the copper droplet are oxidized to form spinel solids, according to the following overall reaction[14,15]:

$$(Cu_2O,CuO)_{slag} + (FeO)_{slag} + (ZnO)_{slag} + (Al_2O_3)_{slag} \rightarrow (Zn^{2+}, Fe^{2+}, Cu^{2+})(Al^{3+}, Fe^{3+})_2O_4 + \text{Cu - alloy droplet}$$

However, the fact that silver is present in the attached copper droplets in this study indicates that the origin of the attachment is not purely reactive, as it is almost impossible that the Ag would dissolve in such large amounts into the slag, as illustrated by the SEM–EDX measurements in Table IV. This is confirmed by the observations of Takeda *et al.*[16] They showed that Ag dissolves slightly into the slag with a distribution coefficient (= pct in slag/pct in Cu-Ag alloy) of the order 10^{-4} to 10^{-2} for partial pressures of oxygen going from 10^{-11} to 1 atm. Note that, even if it were possible for more Ag to dissolve into the slag, this would also not result in precipitation of the Ag, as the equilibrium allows for more Ag to be dissolved, unless the slag drop on the spinel substrate possesses variations in composition or p_{O_2}. Moreover, the concentration of Ag in the small attached metal droplets is too high for the metal droplets to be formed during cooling. Suppose that the attached metal droplets and spinel solids could form during the quench, and suppose that from 100 pct slag with a silver concentration ranging from 0.005 to 0.03 wt pct (according to Takeda *et al.*[16]), 10 pct (volume fraction) Cu droplets are formed (estimated from the microstructure in Figure 7), the attached metal droplet would contain 0.05 to 0.3 wt pct Ag. The concentration of Ag in the attached droplets, however, is higher than 1 wt pct, as shown in Table IV, and increases with increasing concentrations of Ag in the master alloy. A purely dispersive origin can also be excluded, as the silver concentration in the attached metal droplets is always lower than the silver concentration of the master alloys.

It is, therefore, suggested that during the movement of the copper on top of the slag, some Cu-Ag alloy is introduced into the slag phase as small dispersed alloy droplets. However, some Cu also dissolves into the slag under the high-temperature and low oxygen partial pressure conditions and also reduces Fe^{3+} in the slag, creating a locally lower oxygen potential. When this slag mixes with not-yet-reduced slag further away from the interface, dissolved copper is reduced. The small alloy droplets introduced in the slag during the movement of the copper on top of the slag can be considered as heterogeneous nucleation sites, where dissolved Cu can precipitate by reduction of the copper oxide, while the iron oxides in the slag next to the copper droplet are oxidized to form spinel solids, according to the overall reaction (cfr. Supra) as suggested by De Wilde *et al.*[14,15]

A higher amount of Cu was observed in the outer spinel (Table IV), which confirms the above mechanism. Moreover, a higher concentration of Fe was also observed in the outer part of the spinel (Figure 6), which endorses the mechanism suggested further. Furthermore, it was already observed by Scheunis *et al.*[26,27] that spinel solids can form and grow very fast within the slag, which would be essential for the reactive origin of the attachment. However, due to this fast formation, it should be noted that it is possible that a small part of the spinel was formed during the quench, because according to equilibrium calculations, a lower temperature yields a higher fraction of spinel solids.

4. *Alloy droplet–slag interface*

The interface between the large copper alloy droplet and the slag phase, could only be visualized for the 20 wt pct Ag alloy (Figure 8), as all the other samples had no clearly visible interface due to a large amount of pores concentrated at this interface.

The large copper alloy droplet is situated in the lower left corner of the SE image as can also be seen on the elemental Cu and Ag EDX maps. When moving towards the slag phase over the interface, no intermediate phase, such as a copper-oxide phase, was observed. Directly next to the alloy droplet, a slag layer with Si, Pb, Al, and O is found. This slag layer is flanked by a set of spinel solids (consisting of O, Al, Fe, and Zn).

De Wilde *et al.*[15] observed the presence of an intermediate copper oxide layer between the large copper drop and slag phase. They presented two possible explanations for this: a quenching effect or a reaction between the copper and slag. The quenching effect was considered unlikely as the remainder of the microstructure of the sample did not contain any other quench effects such as precipitation out of the slag

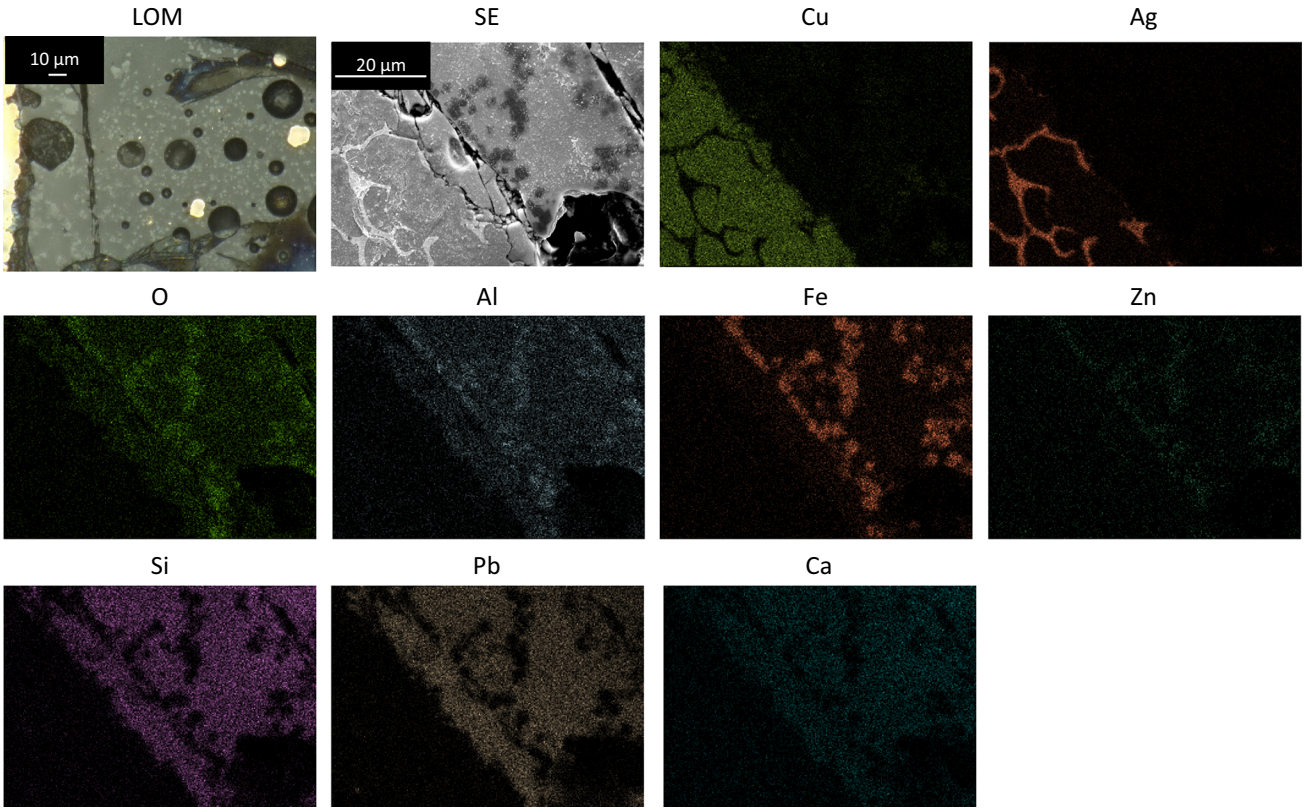

Fig. 8—Optical micrograph, SE image, and elemental map of the interface between the large alloy droplet (20 wt pct Ag) and the slag phase. The scale bar in the SE image and elemental maps are the same.

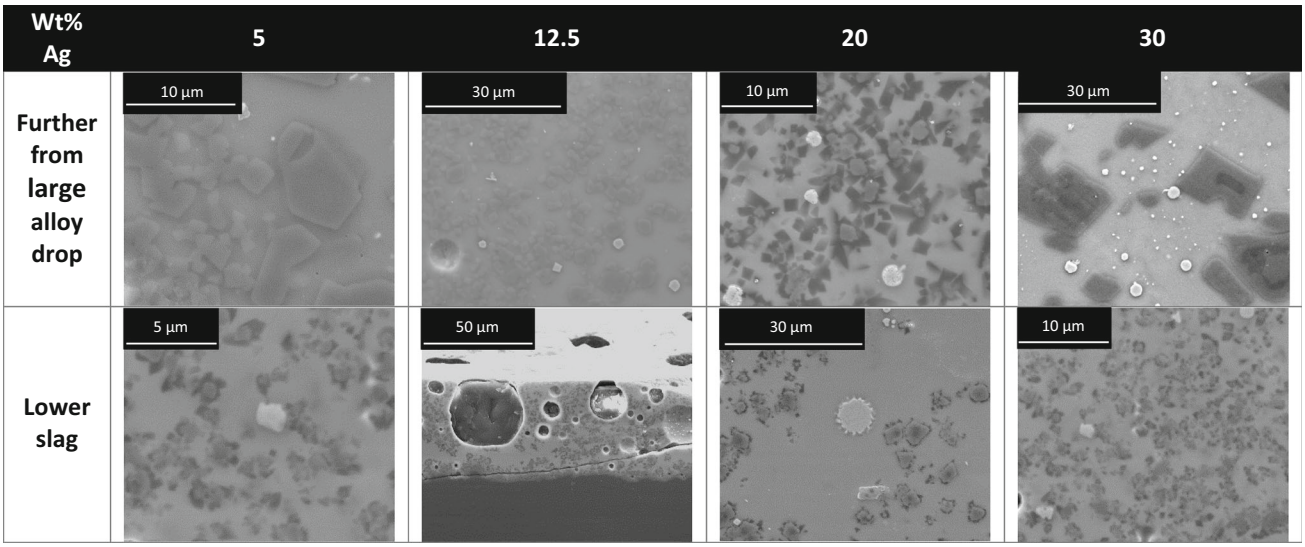

Fig. 9—SE images of the microstructures further away from the large copper alloy droplet and in the lower slag phase for the different Cu-Ag alloys.

matrix. The slag phase in our work also contains a higher amount of Cu with respect to the amount initially present in the slag phase, also indicating the dissolution of the copper alloy drop in the slag. It is possible that the presence of Ag in the copper alloy retarded or stopped the formation of the copper oxide layer at the interface between the two phases. De Wilde *et al.*[10] also found different behaviors between oxygen and Cu-Ag alloys compared to pure copper in sessile drop experiments. As stated by Lee *et al.*[28] and Fima *et al.*,[29] this could be attributed to the accumulation of Ag at the surface, which is then responsible for the different behaviors with oxygen either in the atmosphere in the sessile drop experiments, or in the slag in this study.

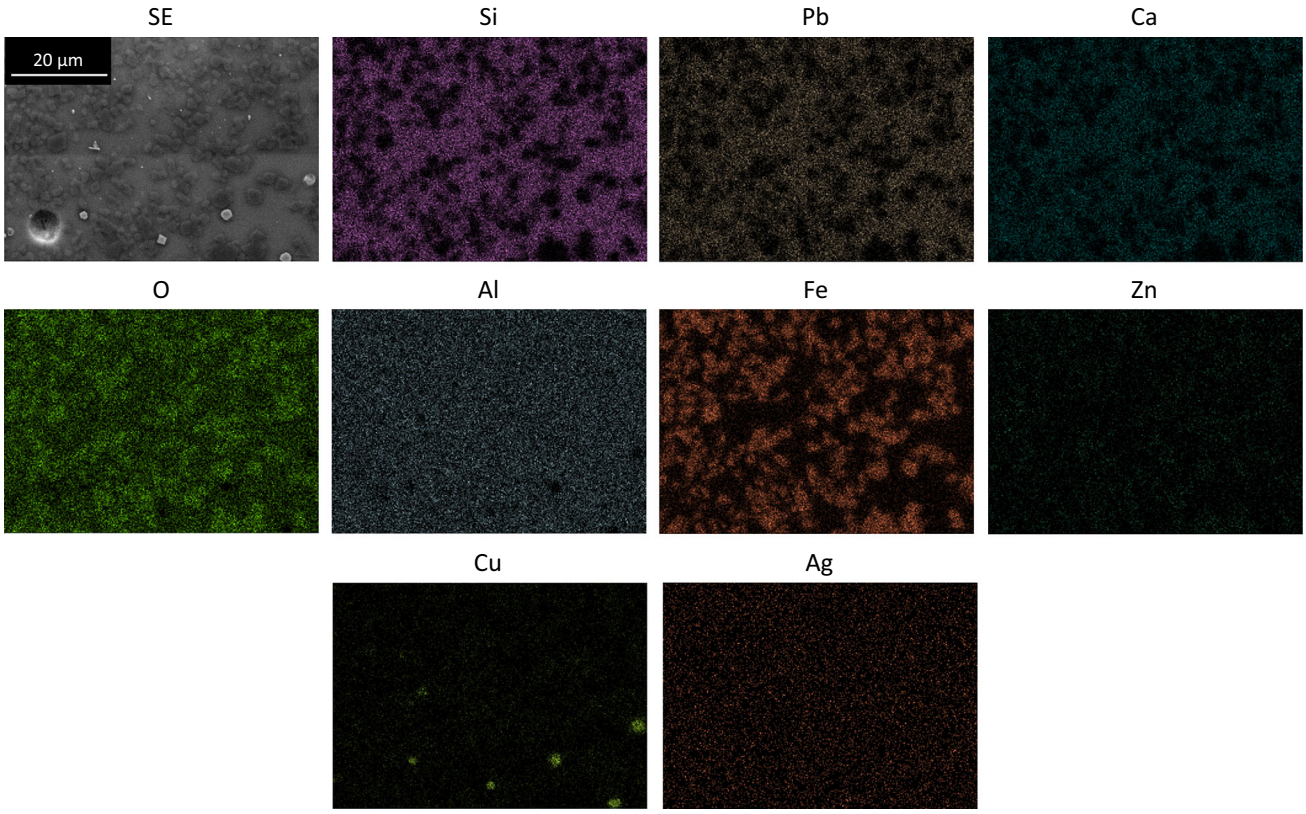

Fig. 10—Elemental map of the microstructure slag further away from the large alloy drop with 12.5 wt pct Ag. The scale bar in the SE image and elemental maps are the same.

Table V. Average Measured Compositions of the Various Phases in the Microstructure Further Away from the Large Alloy Drop for the Different Cu-Ag Alloys

Sample	Phase	Wt Pct Si	Wt Pct Pb	Wt Pct Ca	Wt Pct Mg	Wt Pct O	Wt Pct Al	Wt Pct Fe	Wt Pct Zn	Wt Pct Cu	Wt Pct Ag
5	slag	13.4	14.3	7.2	1.0	30.6	7.9	18.4	4.3	2.7	—
	inner spinel	1.2	1.1	—	1.2	30.3	7.4	49.0	8.2	—	—
20	outer spinel	6.9	3.1	5.3	4.1	35.6	15.6	21.8	6.8	—	—
	attached Cu	5.2	4.4	2.2	—	4.7	3.4	2.0	—	76.1	—
	non-attached Cu	—	—	—	—	—	—	1.2	—	95.8	—
	solids	16.3	8.7	14.1	1.9	35.1	8.3	11.2	—	3.6	—
30	inner spinel	—	—	—	—	30.6	13.4	39.4	14.9	—	—
	attached Cu	1.3	2.5	1.1	—	1.3	—	3.7	1.0	84.5	3.1
	non-attached Cu	—	—	—	—	—	—	2.2	—	91.1	3.2

Compositions below 1 wt pct were assigned with '—'.

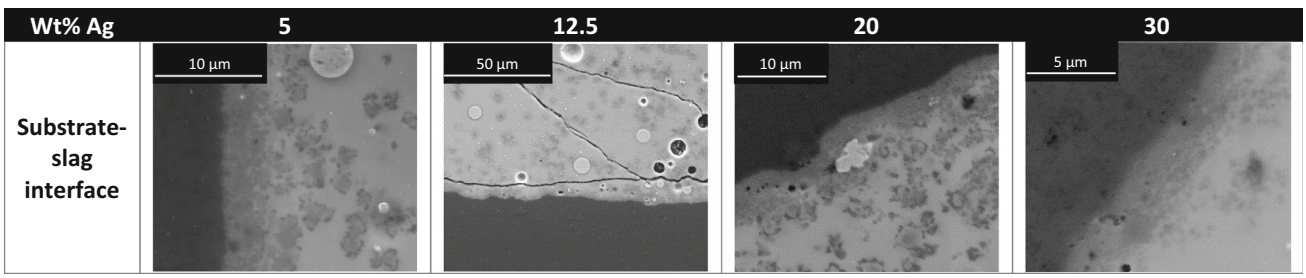

Fig. 11—SE images of the microstructures at the interface between the slag phase and the $MgAl_2O_4$ substrate for the different Cu-Ag alloys.

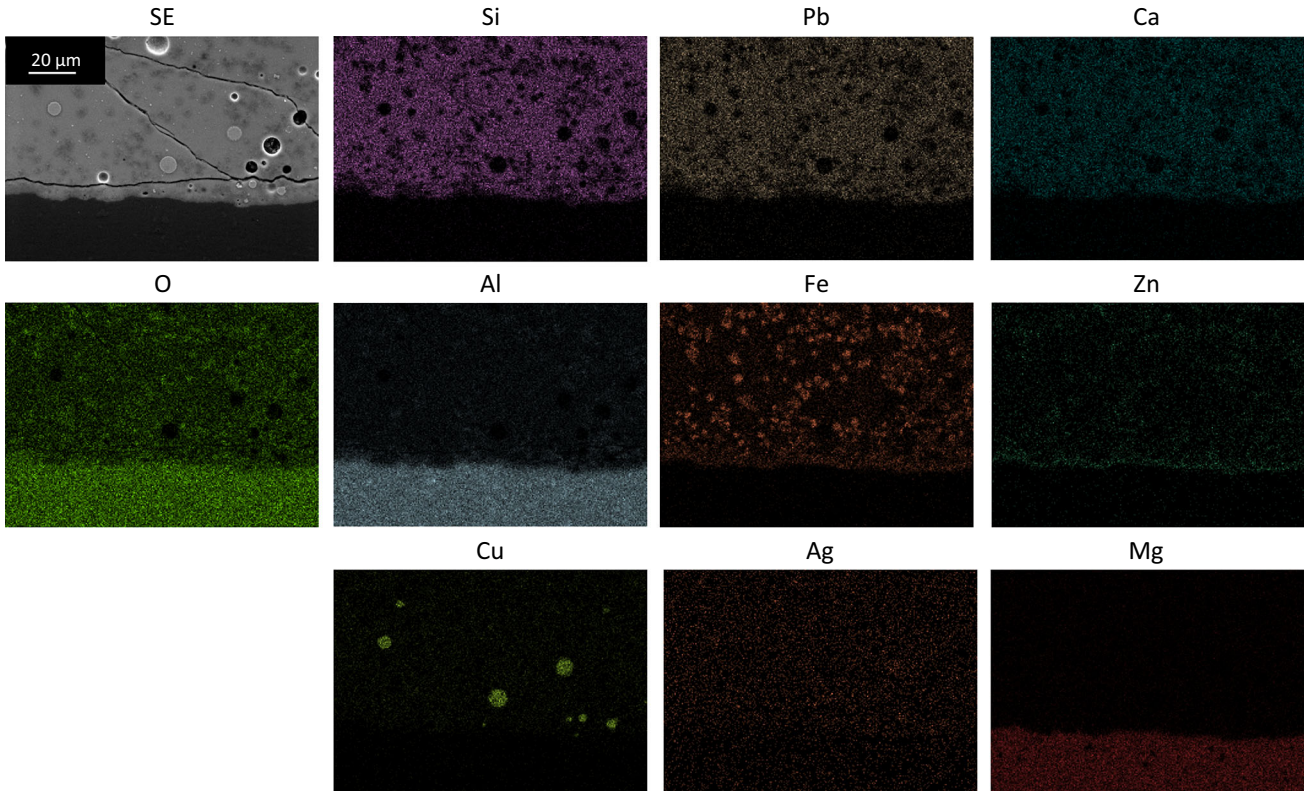

Fig. 12—Elemental map of the microstructure of the slag-substrate interface for the 12.5 wt pct Ag sample. The scale bar in the SE image and elemental maps are the same.

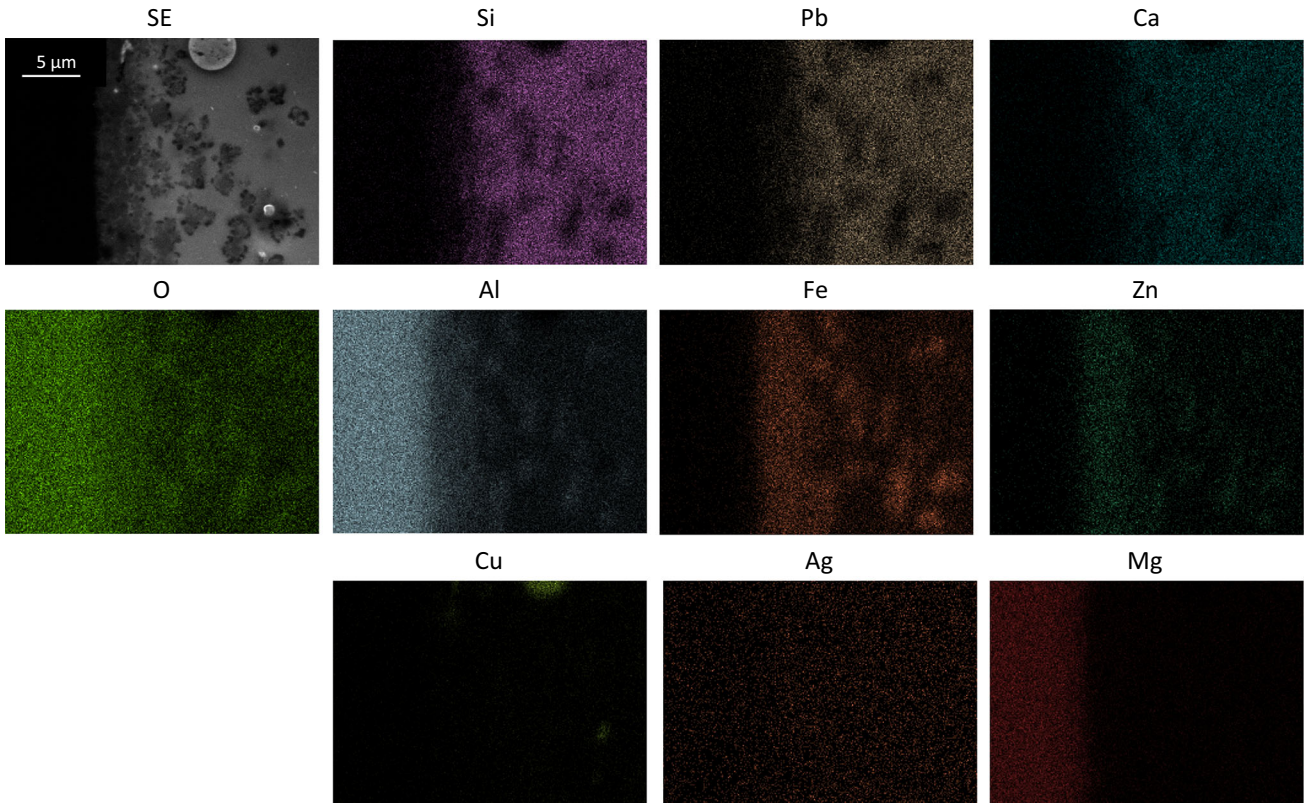

Fig. 13—Elemental map of the microstructure of the slag-substrate interface for the 5 wt pct Ag sample. The scale bar in the SE image and elemental maps are the same.

Table VI. Average Measured Compositions of the Various Phases in the Microstructure at the Interface Between the Slag and the $MgAl_2O_4$ Substrate for the Different Cu-Ag Alloys

Sample	Phase	Wt Pct Si	Wt Pct Pb	Wt Pct Ca	Wt Pct Mg	Wt Pct O	Wt Pct Al	Wt Pct Fe	Wt Pct Zn	Wt Pct Cu	Wt Pct Ag
5	substrate	—	—	—	13.9	43.3	41.9	—	—	—	—
	intermediate layer	2.0	2.5	—	3.5	35.1	24.4	15.0	16.0	—	—
	attached Cu in slag	—	—	—	—	1.9	—	1.0	—	93.6	—
12.5	substrate	—	—	—	14.0	43.0	42.3	—	—	—	—
	intermediate layer	4.0	5.2	1.9	4.3	36.1	22.5	12.4	11.9	1.7	—
	slag	15.0	24.6	8.3	0.7	30.8	6.4	5.3	1.3	7.4	—
	attached Cu in slag	—	—	—	—	—	—	—	—	93.1	2.4
	non-attached Cu in slag	—	—	—	—	—	—	1.2	—	94.0	1.6
20	substrate	—	—	—	15.1	41.3	42.7	—	—	—	—
	intermediate layer	—	—	—	11.1	36.2	34.3	7.6	7.9	1.0	—
	Slag	15.6	20.6	10.0	1.2	31.8	7.4	7.0	1.4	4.7	—
	spinel in slag	14.5	19.4	9.0	—	32.1	7.3	10.2	1.6	4.6	—
	solids in slag	12.5	11.7	9.6	1.9	35.1	9.9	12.6	3.8	2.8	—
30	substrate	—	—	—	14.2	42.3	42.5	—	—	—	—
	intermediate layer	2.5	3.3	1.3	8.2	37.8	28.4	10.5	7.5	—	—
	slag	15.8	22.8	8.7	1.6	32.6	9.4	5.8	—	—	—

Compositions below 1 wt pct were assigned with '—'.

5. *Slag further away from the large alloy droplet*

Further away from the large alloy droplet and in the lower slag phase (closer to the substrate), some attached copper droplets are also observed as shown in Figure 9. However, they are present to a smaller extent in these areas. Moreover, more darker solids are present, as already observed in the slag directly next to the alloy drop for the 20 wt pct Ag case. An elemental map illustrating the distribution of the elements over the different phases in the slag phase further away from the large alloy drop is shown in Figure 10.

The amount of attached metal droplets is lower and the spinel particles seem smaller. The compositions of the different constituents in the microstructures further away from the large alloy drop were measured with EDX and the results are shown in Table V.

The compositions of all phases are very similar to the ones listed in Table IV. The spinel particles are again mainly constituted of O, Al, Fe, and Zn and the same observations can be made regarding the inner and outer spinel parts. The attached metal droplets clearly contain less Cu as more of the other elements (not Cu or Ag) are present within the droplets. Due to the very small dimensions of the darker solids, it is not straightforward to quantify the amounts of Fe and Al precisely and to determine the chemical formula. Based on the composition, it could be suggested that the small darker solids are hedenbergite ($CaFeSi_2O_6$) or esseneite ($CaFeAlSiO_6$), which is in accordance with the findings of De Wilde *et al.*[15] The compositions of the different constituents in the microstructure in the lower slag were measured with EDX and are very similar to the compositions corresponding to the slag phase further away from the large alloy droplet.

6. *Slag–spinel substrate interface*

The large copper alloy drop did not have direct contact with the spinel substrate, but the slag did and a certain interaction between the slag and the spinel substrate could be observed, as shown in Figure 11.

An intermediate layer is formed between the slag and the $MgAl_2O_4$ substrate. The SE image of the 12.5 wt pct Ag sample does not give a clear intermediate layer, but it is present, as confirmed by the elemental map in Figure 12.

The Zn and Fe maps in particular illustrate the presence of the intermediate layer. This is even clearer in a sample with a larger intermediate layer, such as the 5 wt pct Ag sample in Figure 13. Moreover, the EDX measurements of the slag, intermediate layer, and the substrate for all the samples are shown in Table VI.

The substrate consists of Mg, Al, and O and virtually no other elements. It should be noted, however, that the points measured in the substrate were situated at a specific distance from the intermediate layer, where no diffusion processes are expected to alter the substrate composition. The intermediate layer is a spinel solid solution of Mg, O, Al, Fe, and Zn, but with a different composition than the spinel solids in the slag phase. The large difference with the spinel solids in the slag phase is the presence of the Mg. Some non-spinel forming elements (such as Si and Pb) are also measured to a

small amount. The slag phase near the intermediate slag layer contains more Mg than in the other regions of the samples. This Mg can only originate from a diffusion process from the $MgAl_2O_4$ substrates, which indicates its dissolution. Additionally, the amount of Al in the slag is slightly higher next to the interaction layer with respect to the other regions in the samples, which also confirms that the $MgAl_2O_4$ dissolves into the slag. De Wilde *et al.*[15] observed gradients in composition seen on the elemental maps, which could result from the diffusion of Fe and Zn from the slag and intermediate layer into the spinel substrate. However, this is not visible in our results and it should be noted that De Wilde *et al.*[15] also indicated that the gradients in composition seen on the elemental maps could also be due to an interference with the interaction layer.

Both the captured images during the high-temperature CSLM experiment (Figure 2) and the microstructural overview of the samples (Figure 3) demonstrate that the large copper alloy droplet is not in contact with the spinel substrate after the movement of the copper on top of the slag. This agrees with the results of standard sessile drop experiments in literature: copper generally displays a non-wetting behavior on spinel substrates, whereas slags display good wetting on spinel substrates. This good wetting of the slag on the $MgAl_2O_4$ substrate was also observed previously by Abdeyazan *et al.*,[30] Tran *et al.*,[31] and Donald *et al.*[32] Moreover, an interaction layer consisting of (Mg, Zn, Fe)(Al, Fe)$_2O_4$ is formed. This is in accordance with the results of De Wilde *et al.*,[15,18] *i.e.*, that the $MgAl_2O_4$ substrate dissolves into the slag. Due to this dissolution, the concentration in spinel-forming elements becomes very high, inducing the formation of the spinel intermediate layer. They proposed the following reaction taking place at the studied $MgAl_2O_4$-slag interface:

$$\begin{aligned} &MgAl_2O_{4\ \text{solid}} + (Fe_2O_3, FeO, ZnO\ Al_2O_3)_{\text{slag}} \\ &\quad \rightarrow (Mg^{2+}, Zn^{2+}, Fe^{2+})(Al^{3+}, Fe^{3+})_2O_{4\ \text{interaction layer}} \\ &\quad + (MgO)_{\text{slag}} + (Al_2O_3)_{\text{slag}} \end{aligned}$$

Furthermore, this overall reaction was confirmed previously by thermodynamic calculations using FactSage.[18]

IV. CONCLUSION

In this study, the attachment of copper droplets to spinel particles in slags, retaining the sedimentation of the droplets, is studied. Adapted sessile drop experiments were performed, in which both copper alloys and slag were placed on a spinel substrate. Several copper-silver alloys, a synthetic PbO-CaO-SiO_2-Cu_2O-Al_2O_3-FeO-ZnO slag and a $MgAl_2O_4$ substrate, were used to represent the copper alloy droplets, slag, and spinel solids, respectively. The silver was added to the copper alloy as a trace element to get more insights into the origin of the attachment.

The slag displayed a very good wetting behavior on the $MgAl_2O_4$ substrate, whereas the copper alloy drop did not wet the spinel substrate. During the high-temperature CSLM experiment, the slag moved towards the alloy drop and the copper moved rapidly on top of the slag, after which the slag positioned itself between the substrate and the alloy drop. Thus, no direct interaction between the copper and the $MgAl_2O_4$ substrate was possible.

The microstructures within the different samples were studied and the compositions of the different phases present were determined. A (Mg, Zn, Fe) (Al, Fe)$_2O_4$ interaction layer was formed at the slag-$MgAl_2O_4$ interface. At the slag-copper droplet interface, no interaction layer was observed, but copper dissolution into the slag was noted.

Small entrained copper droplets sticking to spinel solids were present within the slag droplet. A mechanism is proposed to explain the presence of those sticking droplets. It is suggested that during the movement of the copper on top of the slag in the high-temperature CSLM experiment, some small Cu-Ag droplets are dispersed within the large slag drop. Some Cu also dissolves into the slag under the high temperature and low oxygen partial pressure conditions. Thus, at one site (the bulk metal/slag interface): $Fe^{3+}_{\text{slag}} + Cu_{\text{metal}} \rightarrow Fe^{2+}_{\text{slag}} + Cu^{+}_{\text{slag}}$. When this slag mixes with not-yet-reduced slag further away from the interface, dissolved copper is reduced. Thus, at the other site (mixing inside the bulk slag): $Fe^{2+}_{\text{slag}} + Cu^{+}_{\text{slag}} \rightarrow Fe^{3+}_{\text{slag}} + Cu_{\text{metal}}$. The previously dispersed Cu-Ag droplets act as nucleation sites for this simultaneous reduction of copper oxides into metallic copper and the oxidation of slag oxides into more stable spinel structures. In this way, the spinel solids grow at the side of the Cu-Ag droplets, which in turn are enriched with Cu and grow. This leads to copper droplets attached to spinel solids within the slag phase.

ACKNOWLEDGMENTS

I. Bellemans holds a Ph.D. fellowship of the Research Foundation - Flanders (FWO).

REFERENCES

1. R. Degel, H. Oterdoom, J. Kunze, A. Warczok, and G. Riveros: *Proceedings of Platinum in Transformation, Third International Platinum Conference*, The Southern African Institute of Mining and Metallurgy, Sun City, 2008, pp. 197–202.
2. I.-K. Suh, Y. Waseda, and A. Yazawa: *High Temp. Mater. Process.*, 1988, vol. 8, pp. 65–88.
3. J.L. Liow, M. Juusela, N.B. Gray, and I.D. Sutalo: *Metall. Mater. Trans. B*, 2003, vol. 34B, pp. 821–32.
4. N. Cardona, P. Coursol, P.J. Mackey, and R. Parra: *Can. Metall. Q.*, 2011, vol. 50, pp. 318–29.
5. I. Imris, M. Sánchez, and G. Achurra: *Miner. Process. Extr. Metall.*, 2005, vol. 114, pp. 135–40.
6. R. Sridhar, J.M. Toguri, and S. Simeonov: *Metall. Mater. Trans. B*, 1997, vol. 28B, pp. 191–200.
7. S.W. Ip and J.M. Toguri: *Metall. Trans. B*, 1992, vol. 23, pp. 303–11.
8. R. Minto and W.G. Davenport: *Can. Min. Metall. Bull.*, 1972, vol. 65, pp. C36–42.
9. L. Andrews: PhD, University of Pretoria, 2008.
10. E. De Wilde, I. Bellemans, M. Campforts, A. Khaliq, K. Vanmeensel, D. Seveno, M. Guo, A. Rhamdhani, G. Brooks, B.

Blanpain, N. Moelans, and K. Verbeken: *Mater. Sci. Technol.*, 2015, vol. 31, pp. 1925–33.
11. I. Bellemans, N. Moelans, and K. Verbeken: *Comput. Mater. Sci.*, 2015, vol. 108, pp. 348–57.
12. I. Bellemans, E. De Wilde, N. Moelans, and K. Verbeken: *Acta Mater.*, 2015, vol. 101, pp. 172–80.
13. I. Bellemans, E. De Wilde, N. Moelans, and K. Verbeken: *Comput. Mater. Sci.*, 2016, vol. 118, pp. 269–78.
14. E. De Wilde, I. Bellemans, L. Zheng, M. Campforts, M. Guo, B. Blanpain, N. Moelans, and K. Verbeken: *Mater. Sci. Technol.*, 2016, vol. 32, pp. 1911–24.
15. E. De Wilde, I. Bellemans, M. Campforts, M. Guo, B. Blanpain, N. Moelans, and K. Verbeken: *Metall. Mater. Trans. B*, 2016, vol. 47B, pp. 3421–34.
16. Y. Takeda, S. Ishiwata, and A. Yazawa: *Trans. Jpn. Inst. Met.*, 1983, vol. 24, pp. 518–28.
17. N. Eustathopoulos: *Acta Mater.*, 1998, vol. 46, pp. 2319–27.
18. E. De Wilde, I. Bellemans, M. Campforts, M. Guo, B. Blanpain, N. Moelans, and K. Verbeken: *Trans. Nonferrous Met. Soc. China*, 2016, vol. 26, pp. 2770–83.
19. N. Eustathopoulos, M.G. Nicholas, and B. Drevet: *Wettability at High Temperatures*, Elsevier, Oxford, 1999.
20. C.W. Bale, P. Chartrand, S.A. Degterov, G. Eriksson, K. Hack, R. Ben Mahfoud, J. Melançon, A.D. Pelton, and S. Petersen: *Calphad*, 2002, vol. 26, pp. 189–228.
21. J.W. Cahn: *Acta Metall.*, 1961, vol. 9, pp. 795–801.
22. P.J. Potts: *Handbook Silicate Rock Analysis*, Springer, Dordrecht, 1987, pp. 226–85.
23. X. Llovet, E. Valovirta, and E. Heikinheimo: *Microchim. Acta*, 2000, vol. 132, pp. 205–12.
24. T. Sakai, S.W. Ip, and J.M. Toguri: *Metall. Mater. Trans. B*, 1997, vol. 28B, pp. 401–07.
25. E. De Wilde, I. Bellemans, M. Campforts, M. Guo, K. Vanmeensel, B. Blanpain, N. Moelans, and K. Verbeken: *J. Sustain. Metall.*, 2017, vol. 3, pp. 416–27.
26. L. Scheunis, M. Campforts, P.T. Jones, B. Blanpain, and A. Malfliet: *J. Eur. Ceram. Soc.*, 2015, vol. 35, pp. 347–55.
27. S.A. Nightingale and B.J. Monaghan: *Metall. Mater. Trans. B*, 2008, vol. 39B, pp. 643–48.
28. J. Lee, T. Tanaka, Y. Asano, and S. Hara: *Mater. Trans.*, 2004, vol. 45, pp. 2719–22.
29. P. Fima and N. Sobczak: *Int. J. Thermophys.*, 2010, vol. 31, pp. 1165–74.
30. H. Abdeyazdan, N. Dogan, M. Rhamdhani, M. Chapman, and B. Monaghan: *Metall. Mater. Trans. B*, 2014, vol. 46B, pp. 208–19.
31. T. Tran, D. Xie, and Y. B. Cheng: *Proceedings of the VII International Conference on Molten Slags, Fluxes & Salts*, The South African Institute of Mining and Metallurgy, 2004.
32. J.R. Donald, J.M. Toguri, and C. Doyle: *Metall. Mater. Trans. B*, 1998, vol. 29B, pp. 317–23.